

ERNST ABBE'S

Theory of Image Formation in the Microscope

ERNST ABBE'S

Theory of Image Formation in the Microscope

Written and published by Otto Lummer and Fritz Reiche under the title
Die Lehre von der Bildentstehung im Mikroskop von Ernst Abbe
Translated and annotated, with additional material,
by Anthony Yen and Martin Burkhardt

SPIE PRESS
Bellingham, Washington USA

Library of Congress Cataloging-in-Publication Data

Names: Abbe, Ernst, 1840–1905, author. | Lummer, O. (Otto), 1860–1925, editor. | Reiche, F. (Fritz), 1883–1969, editor. | Yen, Anthony, translator, annotator. | Burkhardt, Martin, translator, annotator.

Title: Ernst Abbe's theory of image formation in the microscope / written and published by Otto Lummer and Fritz Reiche; translated and annotated, with additional material, by Anthony Yen and Martin Burkhardt.

Other titles: Die Lehre von der Bildentstehung im Mikroskop von Ernst Abbe. English | Ernst Abbe's theory of image formation in the microscope

Description: First printing. | Bellingham, Washington : SPIE, [2022] | "This work was originally published in 1910, five years after Ernst Abbe's death. The original book, published by Friedrich Vieweg und Sohn, was compiled by Otto Lummer, professor of physics at the University of Breslau, and his then-assistant Fritz Reiche" – translators' foreword. | Includes bibliographical references and index.

Identifiers: LCCN 2022021996 | ISBN 9781510655232 (paperback) | ISBN 9781510655249 (pdf)

Subjects: LCSH: Microscopy.

Classification: LCC QH205 .A213 2022 | DDC 570.28/2–dc23/eng/20220720

LC record available at <https://lccn.loc.gov/2022021996>

Published by

SPIE

P.O. Box 10

Bellingham, Washington 98227-0010 USA

Phone: +1 360.676.3290

Fax: +1 360.647.1445

Email: books@spie.org

Web: <http://spie.org>

Copyright © 2023 Society of Photo-Optical Instrumentation Engineers (SPIE)

All rights reserved. No part of this publication may be reproduced or distributed in any form or by any means without written permission of the publisher.

The content of this book reflects the work and thought of the authors. Every effort has been made to publish reliable and accurate information herein, but the publisher is not responsible for the validity of the information or for any outcomes resulting from reliance thereon.

Cover image courtesy of ZEISS Archives.

Printed in the United States of America.

First printing 2023.

For updates to this book, visit <http://spie.org> and type "PM352" in the search field.

SPIE.

Contents

Translators' foreword	VII
Special foreword	XI
Preface	XVII
Introduction	1
1 Imaging laws of geometrical optics	3
1 Construction of a ray refracted by a spherical surface . . .	3
2 Imaging of an arbitrary luminous axial point	6
3 Imaging of luminous objects	7
4 Imaging by a centered system of refracting spherical surfaces	9
5 Imaging equations according to Abbe	10
6 Imaging by wide-angle ray bundles (sine condition) . .	13
2 Imaging of self-luminous objects	21
7 Diffraction problems solved on the basis of Maxwell's theory	21
8 The Kirchhoff principle	23
9 Discussion of expression for the intensity at the observation point	30

10	Comparison of the Kirchhoff principle with the Fresnel–Huygens principle	33
11	Fraunhofer diffraction	35
12	Auxiliary consideration	37
13	Diffraction phenomena occurring in pairs of conjugate planes of optical systems	40
14	Determination of factors α , $\sigma(u)$, and $\psi(u')$ based on energy considerations	44
15	Expression of light disturbance at the observation point	51
16	Determination of light disturbance at the observation point using the Kirchhoff principle	52
17	Calculation of diffraction on an aperture of specific form for points in the plane conjugate to the object plane in the presence of a luminous surface element . .	57
3	Imaging of illuminated objects	65
18	Presence of several luminous points	65
19	Presence of several luminous surface elements	67
20	Single luminous slit	69
21	Two parallel and neighboring slits	73
22	An illuminated slit of finite width	84
23	Finite slit whose two halves possess a constant difference in phase	95
24	Slit of finite width with oblique incidence of light . . .	107
25	Switching of the order of integration in the calculation of the resulting light disturbance	120
26	Pointwise and similar imaging of the object	129
27	Dissimilar imaging of the object	131
4	Imaging of a grating with artificial clipping of diffraction orders	135
28	General intensity equation	135

29	Case I: Only the central image (the 0th order) goes through	137
30	Case II: Besides the central image, the left and right first maxima go through	142
31	Case III: Only the i th maxima on both sides contribute to imaging; the central image is blocked	145
Appendix		149
	Bibliography on the theory of imaging of illuminated objects	149
Translators' notes		151
A brief introduction to geometrical optics		173
On the $0.5\lambda/\text{NA}$ resolution limit in the imaging of periodic patterns		187
	Abbe's 15 December 1876 Letter to J. W. Stephenson	201

Introduction

Geometrical optics assigns reality to light rays and assumes that where light rays intersect is also where light concentration actually occurs. This arithmetic optics seeks accordingly to evaluate optical systems in such a way that two spaces are imaged onto each other point for point; i.e., outgoing rays from one point in one space (object space) reunite at one point in another space (image space). If an optical system meets this condition, it then transforms the outgoing convex spherical wavefront from the object point to a concave spherical wavefront whose center is the image point. Arithmetic optics does not have to deliver any more than this.

In order to understand the actual light distribution in the center of the concave spherical wavefront, i.e., the image point, image formation must be handled based on wave theory as a diffraction problem. One usually expresses the result of this approach by overlaying on the point of convergence of the homocentric ray bundle (image point in geometrical optics) the diffraction phenomenon that is uniquely determined by the type of blocking to the spherical wavefront in the image space. In reality, the process is reversed: the diffraction phenomenon is the primary image-forming process, and the image point is secondary. In fact, the image where the imaging ray bundle is limited by a circular aperture is at best a diffraction disk with alternating dark and bright diffraction rings of rapidly decreasing intensity. The greater the image angle whose sine is given by the ratio of the radius

Chapter 1

Imaging laws of geometrical Opticsⁱⁱ

§1. Construction of a ray refracted by a spherical surface

Let M (Fig. 1) be the center of the refracting sphere of radius r and refractive index n' , and the ambient medium have the refractive index n . To find the refracted ray from the incident ray LE, we insert, according to the elegant method of construction of Weyerstraß, two auxiliary circles 1 and 2 with radii

$$r_1 = \frac{n'}{n}r$$

and

$$r_2 = \frac{n}{n'}r,$$

extend ray LE until it intersects auxiliary circle 1 at A, and connect E with point A' where line AM and auxiliary circle 2 intersect. Line EA'L' is the refracted ray associated with LE.

From the similarity of triangles EAM and EA'M, it follows that

$$\angle MEA = \angle EA'M^{\text{iii}}$$

that follows, we have the theorem: *the object space is imaged point-to-point in the image space. Planes perpendicular to the axis in the object space correspond point-to-point to the planes perpendicular to the axis in the image space.*

If one applies the Lagrange relation to each refracting surface in the system successively, one obtains the Lagrange–Helmholtz relation

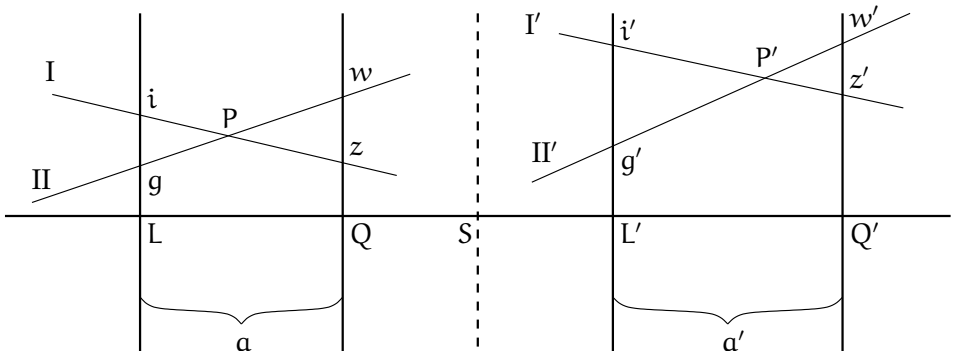
$$\left. \begin{array}{l} \beta \cdot \gamma = \frac{n}{n'} \\ \text{or } y'n' \tan u' = yn \tan u \end{array} \right\}, \quad (5)$$

where β and γ now denote the lateral magnification and angular magnification with respect to the *entire system*, and n and n' are refractive indices of the front (object) and back (image) media.

§5. Imaging equations according to Abbe

In Fig. 6, let there be conjugate pairs of planes L and L' as well as Q and Q', and the associated lateral magnifications be given by

Figure 6



Chapter 2

Imaging of self-luminous objects in terms of wave theory

§7. Diffraction problems solved on the basis of Maxwell's theory

We have seen that a centered system (microscope objective) images a surface element point-to-point and in similarity, using arbitrarily wide-angled ray bundles, only if the sine condition

$$\frac{\sin u'}{\sin u} = \frac{n}{n'} \cdot \frac{1}{\beta}$$

is fulfilled. If the system is so designed that this condition is satisfied, then all incoming rays to any point of the image remain perpendicular to a spherical surface centered on this point.^{xvi} The lens designer^{xvii} cannot offer anything more than this. We wonder whether and under what conditions this purely geometrical, pointwise concentration of rays is also physically present. Let us for the moment remain on the fiction of geometrical optics, that there were actually luminous points, so only the spherical wave emanating from this point would be a reality. Only with free, absolutely unhindered propagation, as would be the case in an arbitrarily extended, homogeneous medium,

trical waves (Großmann⁹). Finally, the diffraction phenomenon on metallic cylinders of elliptical cross section was treated (B. Sieger¹⁰ and K. Aichi¹¹), if only for material of infinitely large conductivity.

§8. The Kirchhoff principle

In general, the treatment of diffraction phenomena according to the Kirchhoff principle gives a far simpler form, allowing then the calculation of cases of our interest. Applying Green's theorems^{xviii} to a function φ , which satisfies the wave equation^{xix}

$$\frac{\partial^2 \varphi}{\partial t^2} = a^2 \Delta \varphi, \quad (12)$$

Kirchhoff¹² obtained the value of the function φ at an observation point P (Fig. 11) as a function of time t in terms of values of φ , $\partial\varphi/\partial t$, and $\partial\varphi/\partial\nu$ on the observation point–enclosing surface Σ with inward normal ν ; here one must, for the magnitudes of φ , $\partial\varphi/\partial t$, and $\partial\varphi/\partial\nu$, insert the values that they possess at position $d\sigma$ at time $t' = t - r/a$, where r denotes the radius vector P $d\sigma$ and a the velocity of light in space V . It is^{xx}

$$\varphi_P(t) = \frac{1}{4\pi} \int_{\Sigma} d\sigma \left[\varphi \frac{\partial(1/r)}{\partial\nu} - \frac{1}{ar} \frac{\partial\varphi}{\partial t} \cdot \frac{\partial r}{\partial\nu} - \frac{1}{r} \frac{\partial\varphi}{\partial\nu} \right]_{t'=t-\frac{r}{a}}. \quad (13)$$

Kirchhoff used this theorem to derive an approximation of the light intensity at observation point P (Fig. 12), if waves originating from L are disturbed by some obstacles. We want to carry out the calculation for the special case of an obstacle that is an *opaque* screen with aperture Σ_1 . For this we place the surface of integration around

⁹Dissertation, Breslau 1909.

¹⁰*Ann. d. Phys.* **23**, 626 (1908).

¹¹*Proc. Tokyo Mathem. Physical Soc.* (2) **4**, 966 (1908).

¹²Kirchhoff, *Lectures on Mathematical Physics, Vol. II, Optics*, 1891 (in German).

or finally,

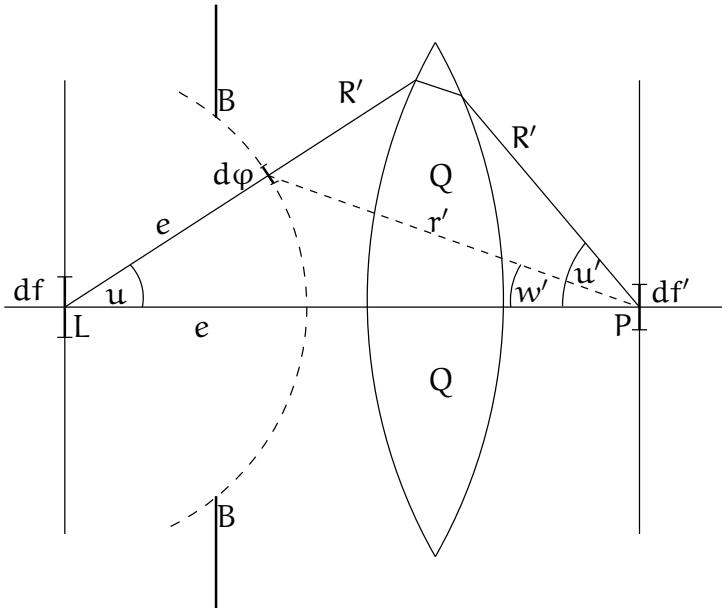
$$\rho = -\frac{x\xi + y\eta}{e}. \quad (17)$$

This simplification of the value ρ for $z = -e$, i.e., for the observation points *that lie in the object plane itself*, acquires a *physical* meaning with the introduction of imaging systems.

§13. Diffraction phenomena occurring in pairs of conjugate planes of optical systems

In Fig. 20, let the surface element df lying at L glow and its image df' , projected by system Q, lie at P. Let diaphragm BB act as the entrance pupil that cuts an effective piece of the surface out of a

Figure 20



which, since e' is large compared to λ' , reduces to the expression identical to Eq. 26,

$$\mathfrak{E}' = \frac{\text{const}}{e'} \cos u' \cdot \cos 2\pi \left(\frac{t}{T} + \frac{e'}{\lambda'} \right).$$

With this it has been shown that \mathfrak{E}' is a solution of the wave equation for the case treated here and therefore can be inserted in place of ϕ in Eq. 13 of the Kirchhoff principle.

If one introduces once again s' via Eq. 24a,

$$J_{P_1} = \overline{\mathfrak{E}'^2} = \overline{s'^2} \cdot \overline{df'},$$

after easy calculation,^{xli} if one replaces r with e' in the amplitude and $\frac{1+\cos u}{2}$ with 1, one obtains

$$\begin{aligned} s' &= \frac{k'}{\lambda'} \int_{\text{II}} \frac{d\varphi' \cos u'}{e'^2} \sin 2\pi \left(\frac{t}{T} + \frac{x'\xi' + y'\eta'}{e'\lambda'} \right) \\ &= \frac{k'}{\lambda'} \int_{\text{II}} \frac{d\xi' d\eta'}{e'^2} \sin 2\pi \left(\frac{t}{T} + \frac{x'\xi' + y'\eta'}{e'\lambda'} \right), \end{aligned}$$

which is exactly the above derived expression (Eq. 24).

It should be pointed out once more that one obtains the "effective piece of boundary surface I" as one draws from the luminous point or surface element all possible rays toward the boundary points on the entrance pupil. The entirety of the intersections of these rays with the spherical surface I form the boundary of the "effective piece." Integration in the expression of s is extended over the projection of this "effective piece" onto the $\xi\eta$ -plane.

§17. Calculation of diffraction on an aperture of specific form for points in the plane conjugate to the object plane in the presence of a luminous surface element

We choose the form of the diffracting aperture in such a way that the projection of the effective piece of the boundary surface onto the $\xi\eta$ -plane is

Chapter 3

Imaging of illuminated objects

§18. Presence of several luminous points

In the presence of *one* luminous surface element, the diffraction pattern is symmetrical with respect to the location of that element. This applies to an arbitrarily located surface element, as long as one limits oneself to points close to the axis of the system. *The diffraction pattern always remains stationary and moves with the luminous surface element.*

With the simultaneous presence of several luminous elements, the observed diffraction pattern depends on whether the individual elements emit independent *incoherent* waves from each other, or whether the waves emitted from individual elements are *coherent*, *i.e.*, capable of interference.

The following laws hold, assuming that we are dealing with several luminous “points”: *If different wave trains are incoherent, one obtains the resulting intensity at each location by simply summing the squares of the amplitudes, i.e., the intensities, that are generated by individual luminous points.*

If n luminous “points” contribute to the light disturbance at the observation point, and if the disturbance generated by their wave trains are represented by the value of the electric field (of the light vector),

$$\begin{aligned}
 A(x) &= \frac{2}{\pi} \int_0^{\frac{2\pi a \alpha'}{\lambda}} dw \cos\left(\frac{xw}{a}\right) \\
 &= \frac{2a}{\pi x} \cdot \sin\left(\frac{2\pi \alpha' x}{\lambda}\right) \\
 &= \frac{4a \alpha'}{\lambda} \cdot \frac{\sin\left(\frac{2\pi \alpha' x}{\lambda}\right)}{\frac{2\pi \alpha' x}{\lambda}}. \tag{56}
 \end{aligned}$$

$A(x)$ has in this case the already discussed form $\frac{\sin v}{v}$. If $\frac{2\pi a \alpha'}{\lambda}$ is very large compared to π , then, as can be seen from the consideration of the form of $\frac{dA(x)}{dx}$, the fluctuations of the amplitude inside the slit are very small, and the value of the amplitude is therefore almost constant; only *at the edges* of the slit do fluctuations take place; namely (if we consider only positive values of x , since the phenomenon is symmetrical with respect to the J -axis), since $\frac{2\pi a \alpha'}{\lambda}$ was already assumed to be large, u is a fortiori large and therefore:

$$\frac{dA(x)}{dx} = -\text{const} \cdot \frac{\sin v}{v}.$$

Therefore, as v gets closer and closer to the value $v = 0$ (as x increases), i.e., $x = a$ (edge of the slit), the fluctuations of $\frac{\sin v}{v}$ begin to become more and more noticeable. We therefore obtain the image of the amplitude indicated in Fig. 42:^{xlix} the larger $\frac{a \alpha'}{\lambda}$ becomes, the more the variations at the edges converge, so that in the limit, for infinitely large $\frac{a \alpha'}{\lambda}$, we obtain the amplitude graph already shown in Fig. 37 above.

§23. Finite slit whose two halves possess a constant difference in phase

Let the slit have width $2a$ and height $2b$; let the phase in the half slit of height $2b$ and width a ($x = -a$ to $x = 0$) be equal to $2\pi \frac{x}{\lambda}$, while

to the grating constant γ . The larger γ becomes, the more diffraction maxima can contribute to image formation, and the greater the similarity. The maximum numerical aperture of a system is reached when $U = 90^\circ$ and is then

$$A = n .$$

Therefore, in this case of *maximum possible performance*,

$$h = n \frac{\gamma}{\lambda_0} . \quad (79)$$

If we denote with h_1 the last diffraction spectrum of intensity or brightness to be considered in the overall image of the function $f(\xi', \eta')$, the system with $A = n$ will image all gratings with absolute similarity, if

$$\gamma \geq \frac{h_1 \cdot \lambda_0}{n} .$$

§27. Dissimilar imaging of the object

We shall base this investigation on a system with maximum aperture $A = n$, which still images a grating with constant γ with absolute similarity, meaning the satisfaction of the inequality

$$\gamma \geq h_1 \lambda_0 / n ,$$

where h_1 is the last diffraction spectrum of intensity still to be considered in the overall image of the function $f(\xi', \eta')$. A grating with a smaller grating constant ($\gamma' < \gamma$) is therefore no longer imaged by the system similarly. If λ_0 has the smallest possible value (photographic waves) and n has the highest possible value (homogeneous immersion), then the grating $\gamma = h_1 \lambda_0 / n$ is imaged in an absolutely similar way (a fortiori all gratings with *larger* grating constants), whereas it is physically impossible to image gratings with smaller grating constants ($\gamma' < \gamma$) similarly.

As an example, let us suppose that $\lambda_0 = 350 \text{ nm}$, $n = 1.65$, and $h_1 = 10$, assuming that maxima with an intensity less than 1 % of the

Chapter 4

Imaging of a grating with artificial clipping of diffraction orders¹

§28. General intensity equation

Finally, as a typical example, we want to treat the imaging of a grating. Let the grating extend along the X-axis from $X = -A$ to $X = +A$, and along the Y-axis from $Y = -B$ to $Y = +B$, so that it lies symmetrically with respect to the X- and Y-axis and let it consist of N slits of width 2α , which are separated by "bars" of width 2Δ . Therefore, $\gamma = 2(\alpha + \Delta)$ is the grating constant. Let N be a large number. Let α' and β' be the angular height and width of the diffracting aperture (boundary), which lies as a whole or in its parts symmetrically to the X- and Y-axis.

¹The results given in this chapter are taken, at our urging, from the doctoral dissertation of M. Wolfke (Breslau 1910), which will soon appear in *Annalen der Physik*.

However, if $\frac{2a}{\gamma} > 0.6$, then the minima of A are positive and yield, after squaring, minima in intensity.

The decrease in intensity from the maximum to the minimum is in the form of a cosine, for it follows the law $I = (1 + C \cos u)^2$, where $u = \frac{2\pi x}{\gamma}$; maxima and minima have equal width (see Figs. 57a and b). We therefore obtain the following result:

If, in addition to the central order, the first two side maxima also contribute to the secondary image, the image shows a structure. The number of grating lines is reproduced correctly in the image, but the intensity drop from the maximum to the minimum is gradual, and the maxima and minima appear equally wide. In addition, under certain circumstances, secondary maxima still occur in the middle of the minima.

§31. Case III: Only the i th maxima on both sides contribute to imaging; the central image is blocked

The expression for intensity now becomes

$$I = \text{const} \cdot 4 \left[\int_{\frac{2\pi a(Ni-1)}{N\gamma}}^{\frac{2\pi a(Ni+1)}{N\gamma}} dw \frac{\sin w}{w} \frac{\sin \frac{N\gamma w}{2a}}{\sin \frac{\gamma w}{2a}} \cos \frac{x}{a} w \right]^2 \quad (96)$$

$$= \text{const} \cdot J_i^2$$

If we introduce a new variable,

$$w_1 = \pi i - \frac{\gamma w}{2a},$$

for the transformation of J_i , the integration limits will become symmetrical with respect to the origin; we can then again omit, as in case II above, the integral over the odd function and finally obtain, after introducing

$$w_2 = \frac{2a}{\gamma} w_1$$

A brief introduction to geometrical optics

Fermat's Principle: Geometrical optics deals with the (artificial) concept of light rays. A light ray from point P to point P' is a P - and P' -containing path s that is always perpendicular to the successive wavefronts of the light as it propagates from P and P' . The optical length, which is the cumulative phase, is then equal to $\int_P^{P'} n ds$, where n is the index of refraction along the path. Being perpendicular to the two neighboring wavefronts, ds is the shortest distance between them. Therefore, if l is any other path connecting points P and P' , it must be that

$$\int_P^{P'} n ds \leq \int_P^{P'} n dl .$$

This is the same as stating that the optical length $\int_P^{P'} n ds$ from points P to P' is a stationary one. This is called Fermat's principle. To find the actual ray path, we start by considering an arbitrary path from P to P' , vary it while holding the two ends fixed, and set the variation $\delta\left(\int_P^{P'} n dl\right)$ to zero.



Anthony Yen is Vice President and Head of the Technology Development Center at ASML, responsible for providing the company with mid- and long-term directions in semiconductors and working with customers, peers, universities, and research centers to develop enabling technologies. Prior to joining ASML, he headed the Nanopatterning Technology Infrastructure Division at TSMC and played a key role in developing EUV lithography for high-volume production. He received his undergraduate degree in electrical engineering from Purdue University and his master's, engineer's, doctoral, and MBA degrees from MIT. He is a Fellow of SPIE, a Fellow of IEEE, a recipient of the Frits Zernike Award for Microlithography from SPIE, and a recipient of the Outstanding Electrical and Computer Engineer Award from Purdue.



Martin Burkhardt is a Research Staff Member at IBM Research in Yorktown Heights, NY. He has worked in lithography since leaving graduate school, first at Texas Instruments, then at ASML, before joining IBM in 2001. Starting with i-line lithography, he now works on imaging and mask technologies for EUV lithography, following the shrinking wavelengths that were used in state-of-the-art lithography for integrated circuits over the years. He received a Dipl.-Ing. degree from the Technical University of Berlin, and a Ph.D. from MIT, both in electrical engineering. He is a Fellow of SPIE.